Ceramics International 43 (2017) 12557–12562

Contents lists available at ScienceDirect

Ceramics International

journal homepage: www.elsevier.com/locate/ceramint

An efficient SO_2-adsorbent from calcination of natural magnesite

Qiang Zhang[a,b], Qi Tao[a,c,*], Hongping He[a], Hongmei Liu[a], Sridhar Komarneni[c,**]

[a] CAS Key Laboratory of Mineralogy and Metallogeny & Guangdong Provincial Key Laboratory of Mineral Physics and Materials, Guangzhou Institute of Geochemistry, Chinese Academy of Sciences, Guangzhou 510640, PR China
[b] University of Chinese Academy of Sciences, Beijing 100049, PR China
[c] Materials Research Institute and Department of Ecosystem Science and Management and 204 Materials Research Laboratory, The Pennsylvania State University, University Park, PA 16802, USA

ARTICLE INFO

Keywords:
Magnesite
Calcination
SO_2-adsorbents
SO_2 adsorption capacity
Adsorption mechanism
MgO

ABSTRACT

MgO-based adsorbents were prepared by controlling the temperature of magnesite calcination, and the adsorption mechanism of SO_2 and these adsorbents were investigated. The obtained adsorbents were characterized by a combination of characterization techniques, including X-ray diffraction (XRD), transmission electron microscopy (TEM), N_2 adsorption/desorption analysis and Hammett indicator method. XRD patterns and TEM images revealed that a complete decarbonation of $MgCO_3$ occurred at ca. 650 °C, and the crystallinity and crystal size of MgO increased with the increase of calcination temperature. The maximum specific surface area (S_{BET} = 69.6 m^2/g) was obtained for the sample calcined at 650 °C (M-650), which also had the maximum value of base site density as revealed by the Hammett indicator tests. The adsorption capacity of adsorbents towards SO_2 increased with the increase of the base site density and M-650 with the highest base site density displayed the maximum adsorption capacity. The adsorption of SO_2 onto MgO was mainly chemisorption, resulting in the formation of magnesium sulfite and magnesium sulfate on the surface of MgO-based adsorbents, as indicated by X-ray Photoelectron Spectroscopy (XPS) and Fourier Transform Infrared (FTIR) spectra. The chemically bound SO_2 could be desorbed at ca. 435 °C as revealed by thermal analysis under N_2. This study suggests that calcination of naturally occurring magnesite is highly amenable to obtain efficient SO_2 adsorbents.

1. Introduction

Atmospheric pollution is one of the most serious environmental issues in many developing countries, which leads to acid rain, photochemical smog, haze etc. [1]. SO_2 is a typical acidic gas and it is a major contributor to acid rain and fine particles in haze and smog, which can cause serious health hazards like severe irritation of the skin and the respiratory system [2]. This toxic gas is frequently released by the burning of sulfur containing fossil fuels [3]. Increasing traditional energy production in many countries by burning coal due to increased demand keeps pushing up the emission quantity of SO_2 resulting in serious environmental pollution. Hence, great efforts should be made to develop and improve SO_2 removal techniques by adsorption and other methods. Therefore, it is imperative to design efficient and cost-effective adsorption materials.

During the last several decades, some effective techniques have been developed for the removal of SO_2, such as wet flue gas desulfurization (FGD), dry FGD and semidry FGD [4–7]. Among these processes, limestone (lime) is one of the most extensively adopted regents for wet FGD because of its high SO_2 removal efficiency and reliability [8]. Nevertheless, the desulphurization by-product (calcium sulfate) is apt to cause scale formation and subsequent pipe blockage due to its low solubility. A large amount of water is needed in this process and therefore considerable amount of wastewater would be produced and this waste water may easily cause secondary pollution. These drawbacks increase costs of industrial equipment maintenance and bring extra complexity to the desulphurization system. Hence, dry methods and catalytic processes for SO_2 removal have attracted much interest due to the economic benefit and simple operation [9]. Some common adsorbents such as activated carbon, zeolite, metal oxides like CaO, MgO, ZnO, Al_2O_3, Fe_2O_3 etc. have already been used in these processes [1,10–12]. Among these, CaO-based adsorbents have been the main candidate materials in the industrial process during the last several decades. The long-standing problem for this family of adsor-

* Corresponding author at: CAS Key Laboratory of Mineralogy and Metallogeny & Guangdong Provincial Key Laboratory of Mineral Physics and Materials, Guangzhou Institute of Geochemistry, Chinese Academy of Sciences, Guangzhou 510640, PR China.
** Corresponding author.
E-mail addresses: taoqi@gig.ac.cn (Q. Tao), komarneni@psu.edu (S. Komarneni).

http://dx.doi.org/10.1016/j.ceramint.2017.06.130
Received 15 May 2017; Received in revised form 16 June 2017; Accepted 20 June 2017
Available online 21 June 2017

bents is the low desulfurization efficiency [13]. Recently, MgO-based adsorbents have attracted a great deal of interest due to their high efficiency for SO_2 removal. These kinds of adsorbents can be prepared by co-precipitation [14], sol-gel procedure [15], chemical vapor deposition [2], hydrothermal process [16] and thermal decomposition route [17,18]. However, most of these methods are relatively complex and/or with a high cost, which hindered their wide application in industry. Therefore, a simple and economical method is still necessary for the preparation of MgO-based adsorbents.

There is more than 10 billion tons of magnesite reserves in the world. Most of them are distributed in China, North Korea, Russia and Slovakia [19]. Therefore, thermal decomposition of natural magnesite ($MgCO_3$) is an attractive technique to prepare MgO-based adsorbents, considering its abundance in nature, low cost and high Mg content. The calcined products of natural magnesite have been widely used in various industries, such as refractories and cements, as well as rubber and plastics filler, food additives, and environmental materials (desulfurizer in wet-FGD and neutralizing reagent used in acid water treatment) [20,21]. However, only a limited amount of research has been reported on the effect of preparation process of MgO from naturally occurring magnesite for SO_2 adsorption and the SO_2 adsorption mechanism by such MgO.

In this study, MgO-based adsorbents were prepared by calcination of natural magnesite. The morphologies and surface properties of the adsorbents were investigated by a combination of characterization techniques including X-ray diffraction (XRD), Transmission electron microscopy (TEM), N_2 adsorption/desorption analysis and Hammett indicator method. Based upon these results, the SO_2 adsorption reactivity of the obtained adsorbents was evaluated and a possible adsorption mechanism was proposed. The simplicity and potential cost-effectiveness of the MgO adsorbent prepared here may enable its potential industrial applications for SO_2 removal.

2. Experimental part

2.1. Materials

Natural magnesite ore from Dashiqiao, Liaoning Province, China, was used as the raw material. The chemical and phase compositions (Table 1 and Fig. 1) were determined by using X-ray fluorescence (XRF) and X-ray diffraction (XRD) analyses, respectively.

2.2. Preparation of adsorbents

The ore was crushed and sieved to −150 μm before the thermal treatment. The thermal decomposition of the raw materials was carried out in a muffle furnace (Carbolite RHF14/3) at temperatures of 500, 600, 650, 700, 800 and 900 °C for 1 h with a heating rate of 10 °C/min. After cooling to ambient temperature, the obtained adsorbents were marked as M-500, M-600, M-650, M-700, M-800, and M-900 for samples heated at temperatures of 500, 600, 650, 700, 800 and 900 °C, respectively and were stored in desiccator with silica gel before further use.

2.3. Adsorption capacity measurements

The adsorption capacity tests were carried out in a vacuum desiccator (ID = 210 mm). Firstly, a constant mass of adsorbent (1.0000 ± 0.01 g) was paved to a uniform and thin layer on the bottom of the weighing bottles. These open bottles were then put into the vacuum desiccator. Subsequently, the vacuum desiccator was sealed and vacuumed to −0.08 MPa followed by exposure to different partial pressures of dry air and pure SO_2 gas (1:1), which was let in through an inlet until the internal pressure reached constant atmospheric pressure. Thereafter, this desiccator was placed in a room where the temperature was kept constant at 25 °C. The mass increments were measured after different adsorption times to determine the adsorption capacity of the adsorbents.

Table 1
Chemical composition of the natural magnesite (*wt*%).

Element	MgO	CaO	Al_2O_3	SiO_2	MnO_2	Fe_2O_3	L.O.I.[a]
Mass percentage	44.82	1.01	0.21	3.57	0.06	1.71	49.15

[a] L.O.I.: Loss on ignition at 1000 °C.

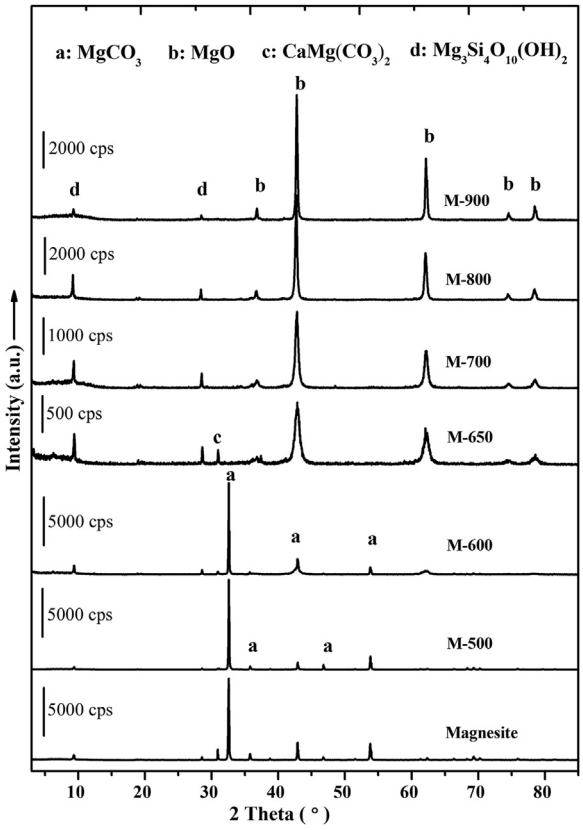

Fig. 1. XRD patterns of natural magnesite and obtained adsorbents. Crystalline phases are designated as: (a) $MgCO_3$ (JCPDS 8–479), (b) MgO (JCPDS 65–476), (c) $CaMg(CO_3)_2$ (JCPDS 36–426), and (d) $Mg_2Si_4O_{10}(OH)_2$ (JCPDS 29–1493).

2.4. Sample characterization

The chemical composition of natural magnesite was analyzed by XRF (Axios, PW4400). XRD patterns were recorded on a Bruker D8 advance diffractometer using Cu Kα radiation scanning from 3 to 85° at a step of 2°/min, operating at 40 kV and 40 mA. Transmission electron microscopy (TEM) observations were performed on a 200 kV JEOL JEM-2100 high-resolution transmission electron microscope. Specific surface area (SSA) was measured by N_2 adsorption/desorption isotherms at 77 K and SSA was calculated using Brunauer, Emmett and Teller (BET) equation. The N_2 isotherms were obtained on an ASAP 2020 instrument. The samples were previously outgassed for 8 h at 200 °C. Hammett indicator method was used to evaluate the base sites density of the adsorbents, using benzoic acid ethanol solution as titrant standard solution based on bromothymol blue indicator (pKa = 7.2).

The thermogravimetric-Fourier transform infrared (TG-FTIR) analysis was conducted on a NETZSCH STA 449F3 thermal analyzer coupled with a Bruker Vertex-70 Fourier-transform infrared spectrometer. Approximately 10 mg of sample was heated from 30 to 800 °C at a rate of 10 °C/min under a highly pure N_2 atmosphere. After heating the evolved gases of samples from TG passed through the FTIR cell to

obtain absorbance information at different wavenumbers. Chemical species of S 2p adsorbed on the surface of adsorbent was analyzed by X-ray photoelectron spectroscopy (XPS) on a Thermo Scientific K-Alpha instrument with monochromatic Al Kα X ray (1486.6 eV) excitation source, using a spot size of 400 μm diameter aperture. For FTIR analyses, adsorbent with absorbed SO_2 was first mixed with KBr powder and pressed into pellet. Then, FTIR spectra of adsorbent with absorbed SO_2 were recorded on a Bruker Vertex-70 FTIR spectrometer using the pressed KBr pellets. The spectra were collected over the range of 900–1700 cm^{-1} with 64 scans and at a resolution of 4 cm^{-1}.

3. Results and discussion

3.1. The crystalline structure and surface properties of the adsorbents

Natural magnesite is one of the Mg-rich carbonate minerals. During calcination, magnesite decomposes as indicated by the following reaction:

$MgCO_3 \rightarrow MgO+CO_2\uparrow$

The formation of MgO crystallites in obtained adsorbents and the relationship between crystallite size and calcination temperature (500–900 °C) were investigated by XRD analysis (Fig. 1). XRD patterns displayed that $MgCO_3$ (JCPDS 8-479) was the main phase in the samples of M-500 and M-600, while in M-600, weak MgO reflections also emerged. MgO (JCPDS 65-476) appeared with the disappearance of magnesite reflections when the calcination temperature reached 650 °C, indicating the decomposition of magnesium carbonate. The intensities of MgO reflections obviously increased with the increase of calcination temperature, reflecting the growth of MgO crystallites [22]. There were two main impurity phases in the raw materials, i.e. dolomite (JCPDS 36-426) and talc-2M (JCPDS 29-1493). The dolomite disappeared when the temperature was above 700 °C, while the talc-2M was kept unchanged during the whole calcination process because of its higher stability than either magneste or dolomite.

During the heat treatment morphological as well as the crystal size changes of MgO were expected to occur. Such changes of MgO in M-650 and M-900 samples were examined by TEM (Fig. 2). A well-crystallized material in the image of M-500, was confirmed by the single crystal-like electron diffraction pattern (see inset in Fig. 2 image of M-500) of crystalline $MgCO_3$ based on the XRD results (Fig. 1). As for the M-650 sample, a kind of morphological moire with indistinct border was clearly visible. Many researchers named it as “pseudomorph” [23,24]. In fact, it was MgO nanocrystallite aggregates which hold the contour of the original particles. This type of pseudomorph possesses large structural defects. Therefore, it can be easily deduced that it was a type of highly reactive MgO. Moreover, a ring-type electron diffraction pattern was also recorded for the M-650, implying the emergence of small crystal of MgO. With increase of calcination temperature (M-900 image in Fig. 2), larger nanocrystalline structure with plate like shaped crystals, which formed by the sintering of small MgO nanocrystallites. These results are in good agreement with those as shown by XRD patterns (Fig. 1).

The effect of phase and crystal size changes on the surface area property of the obtained adsorbents was measured by N_2 adsorption/desorption analysis. The BET specific surface areas calculated from the N_2 adsorption isotherms showed an abrupt increase from M-500 (5.0 m^2/g) to M-650 (69.6 m^2/g) (Table 2). This increase was a result of the phase transformation of magnesium carbonate to the poorly crystallized MgO. However, further increasing the temperature above 650 °C led to a decrease in the specific surface areas from 69.6 m^2/g (M-650) to 17.4 m^2/g (M-900) due to the crystallization of MgO (Table 2).

As a typical solid base, the surface reactivity of MgO was closely related to its base site density on the surface. The Hammett indicator

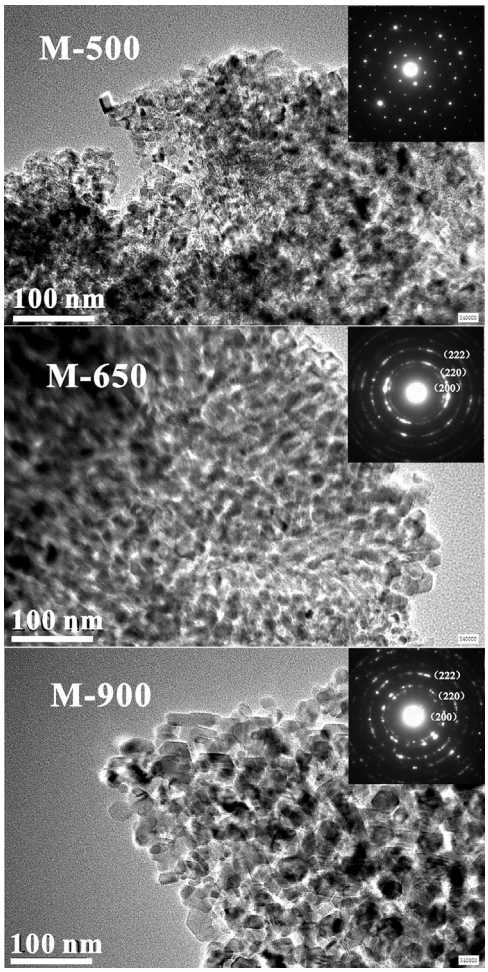

Fig. 2. TEM images and selected area electron diffraction patterns of adsorbents heated at 500, 650 and 900 °C, i.e., M-500, M-650 and M-900 samples, respectively.

Table 2
BET specific surface areas of the obtained adsorbents.

Samples	Magnesite	M-500	M-600	M-650	M-700	M-800	M-900
Specific surface area (m^2/g)	1.1	5.0	32.3	69.6	65.1	25.6	17.4

tests showed that the base site density (pKa≥7.2) significantly increased with the increase of temperature from 500 to 650 °C (Fig. 3). A maximum value of 0.61 mmol/g was reached at 650 °C in the M-650 sample and then decreased gradually to 0.19 mmol/g at 900 °C in the M-900 sample. This tendency is very similar with the variation of specific surface areas (Table 2), and it would certainly have an effect on the adsorption properties of the obtained adsorbents.

3.2. SO_2 adsorption capacity of adsorbents

The adsorption capacity of adsorbents increased with the calcination temperature up to 650 °C reaching a maximum value of 140.7 mg/g (Fig. 4). The obtained results suggested that the base site density on the adsorbent surface was the key factor to control the adsorption capacity because the maximum adsorption correlated with the maximum base site density. Gradual changes of adsorption capacity occurred with time as follows: the adsorption capacity reached 79.5 mg/g in the first period of 1 h (M-650), and then increased

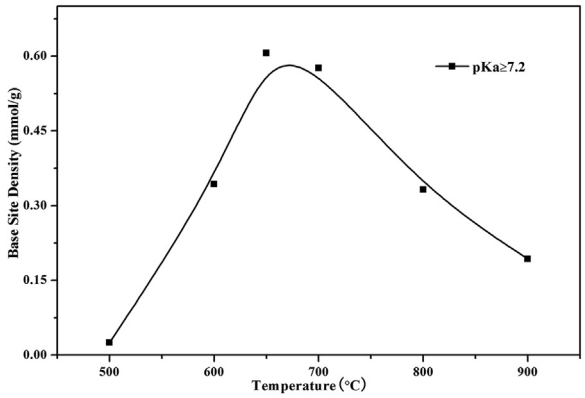

Fig. 3. Base site density of the differently obtained adsorbents.

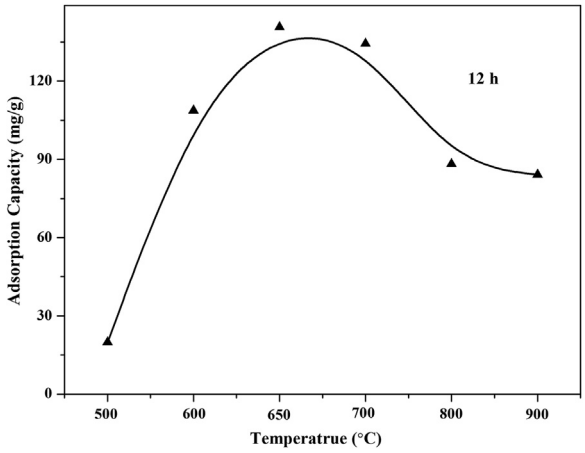

Fig. 4. The Effect of calcination temperature on the adsorption capacity of the obtained adsorbents.

gradually within the following 14 h (Fig. 5). The increment was only 1.6 mg/g from 12 to 15 h, which was much smaller than that from 9 to 12 h (11.2 mg/g). This suggested that a saturation of adsorption of SO_2 could be reached at about 12 h.

3.3. Adsorption mechanism

To elucidate the adsorption mechanism, thermogravimetric analysis was carried out on M-650 sample after adsorption of SO_2 (Fig. 6). The TG and DTG curves displayed three mass loss stages at 133.9, 435.3 and 712.4 °C. The released gases in each stage were detected by

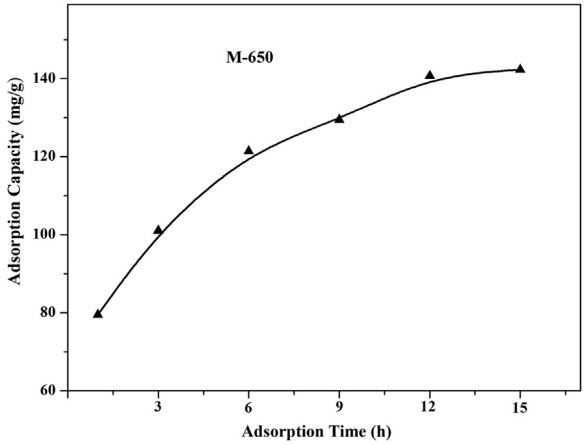

Fig. 5. The influence of adsorption time on the adsorption capacity of M-650 sample.

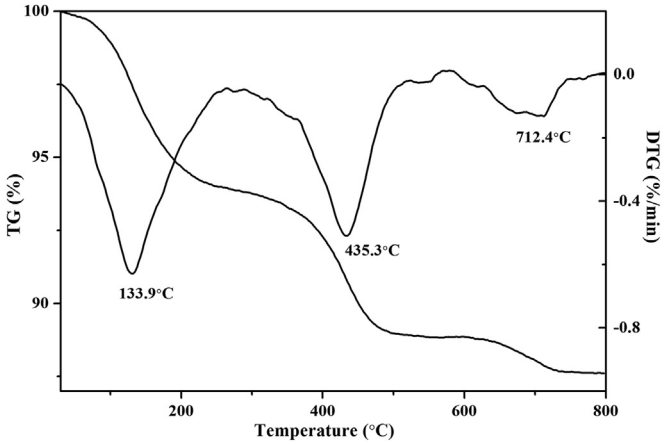

Fig. 6. TG/DTG curve of the M-650 sample with adsorbed SO_2.

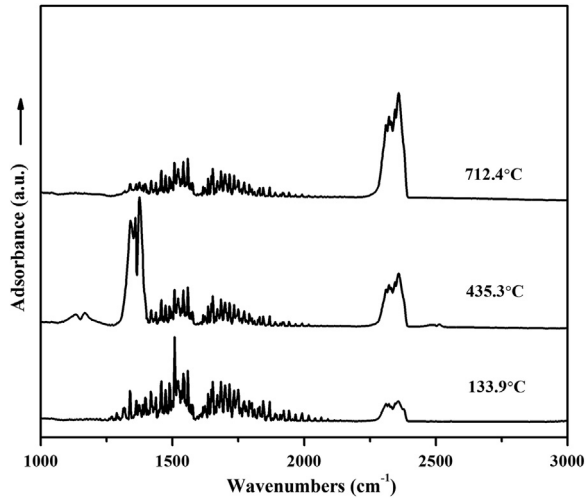

Fig. 7. FTIR spectra of the released gas during the thermal decomposition.

in-situ Fourier-transform infrared spectroscopy (Fig. 7). The results showed that the gases released at the first stage corresponded to bending vibration of vaporous water at 1300–2000 cm^{-1} and asymmetry stretching vibration of CO_2 at 2359 and 2338 cm^{-1}. The second stage (at ca. 435.3 °C) was attributed to release of SO_2, because there were the asymmetrical stretching vibrations and symmetrical stretching vibrations of SO_2 displayed in the regions of 1320–1395 and 1096–1211 cm^{-1} in the FTIR spectrum [25]. At the last stage, the peaks at 2359 and 2338 cm^{-1} intensified, which was possibly as a result of the CO_2 release from decomposition of dolomite. The higher temperature of SO_2 release suggested that there was a chemical bonding between SO_2 and M-650 surface rather than physical bonding.

The chemical species of sulfur for the M-650 with adsorbed SO_2 were further investigated by XPS technique (Fig. 8). The signal of S 2p suggested that this sample contained two chemical species located at ca. 169.2 and 167.4 eV. The 169.2 and 167.4 eV positions could be attributed to the characteristic binding energies for sulfates and sulfites [26]. Thus, these results indicated the formation of magnesium sulfate and sulfite on the MgO surface after SO_2 adsorption. Considering that the oxidation of magnesium sulfites is a spontaneous reaction ($\Delta_r G_m$(25 °C) = −452.9 kJ/mol) [27], it could be concluded that the sulfate resulted from the oxidation of magnesium sulfites in the air/SO_2 mixture.

These processes were further evidenced by the FTIR spectra (Fig. 9). The band at 1023 cm^{-1} corresponded to asymmetrical stretching of Si-O-Si, arising from talc-2M as an impurity mineral, while the peak at 1636 cm^{-1} was attributed to the –OH bending

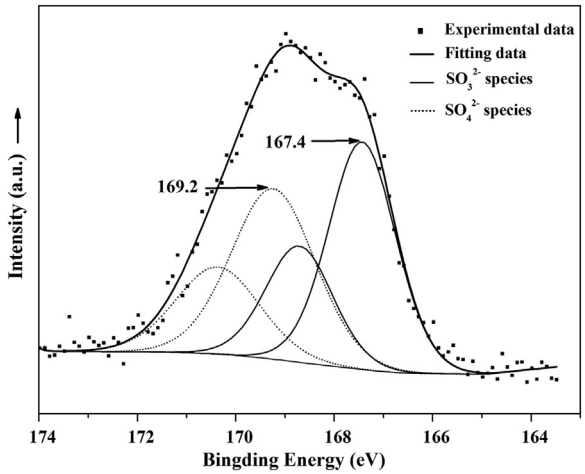

Fig. 8. The peak fitting of the XPS S 2p line of M-650 sample with adsorbed SO_2.

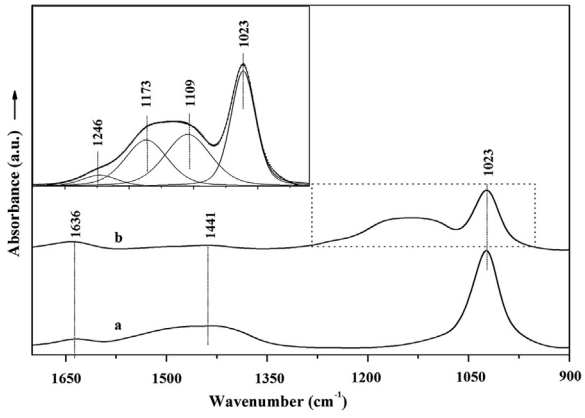

Fig. 9. FTIR spectra of (a) M-650 sample, and (b) M-650 sample with adsorbed SO_2.

vibrations due to the physically adsorbed moisture on the surface of adsorbent. The frequency at 1441 cm^{-1} corresponds to the asymmetric stretching vibration of adsorbed CO_2 and CO_3^{2-} from the undecomposed dolomite [28]. After SO_2 adsorption, its intensity obviously decreased probably due to the replacement of CO_2 by SO_2. Meanwhile, a new broad band was observed at 1075–1300 cm^{-1}, which could be ascribed to the S-O vibration, confirming the formation of sulfur species on the surface of MgO. The deconvolution of the broad band displayed three bands at ca. 1109, 1173 and 1246 cm^{-1}, respectively. The band at 1109 cm^{-1} was attributed to the O-S-O asymmetrical stretching vibration of bidentate sulfite. This kind of bidentate sulfite tends to be formed at high SO_2 partial pressure (0.5 atm) in a mixed gas with a long contact time (12 h) between SO_2 and the adsorbent [29]. While the other two vibrations resulted from the O=S-O and O=S=O asymmetrical stretching of sulfate. The formation of the bidentate sulfite and sulfate on the MgO surface could well explain the SO_2 desorption at higher temperature.

4. Conclusions

An efficient SO_2 adsorbent was prepared by calcination of natural magnesite. The calcination temperature is a key factor to control the surface base site density and consequently the SO_2 adsorption capacity of the obtained adsorbents. XRD patterns and TEM images revealed that a complete decarbonation of $MgCO_3$ occurred at ca. 650 °C, and the crystallinity and crystal size of MgO increased with the increase of calcination temperature. Accordingly, the sample treated at 650 °C (M-650) showed the maximum BET specific surface area, base site density and adsorption capacity towards SO_2, indicating a positive relationship among the three parameters.

The thermogravimetric analyses of the M-650 with adsorbed SO_2 displayed three different mass loss stages, corresponding to the losses of aqueous vapor at ca. 133.9 °C, SO_2 at ca. 435.3 °C and CO_2 at ca. 712.4 °C. This suggested that the adsorbed SO_2 was chemically bound on the MgO surface, where magnesium sulfite and magnesium sulfate was formed as evidenced by XPS spectra. Our present study revealed that chemisorption was mainly involved in the interaction between MgO–base adsorbents and SO_2 rather than physical adsorption. Efficient and potentially cost-effective adsorbents for SO_2 removal in waste gases could be prepared by calcination of magnesite.

Acknowledgements

The financial supports were from the National Natural Science Foundation of China (No. 41372048) and the Foshan-Chinese Academy of Sciences Cooperation Project (No. 20111071010019).

References

[1] E. Atanes, A.N. Marquez, A. Cambra, M.C. Perez, F.F. Martinez, Adsorption of SO_2 onto waste cork powder-derived activated carbons, Chem. Eng. J. 211–212 (2012) 60–67.
[2] J.A. Rodriguez, T. Jirsak, A. Freitag, J. Larese, A. Maiti, Interaction of SO_2 with MgO(100) and Cu/MgO(100): decomposition reactions and the formation of SO_3 and SO_4, J. Phys. Chem. B 104 (2000) 7439–7448.
[3] A. Pieplu, O. Saur, J.C. Lavalley, O. Legendre, C. Nedez, Claus catalysis and H_2S selective oxidation, Catal. Rev. 40 (1998) 409–450.
[4] R.A. Pandey, R. Biswas, T. Chakrabarti, S. Devotta, Flue gas desulfurization: physicochemical and biotechnological approaches, Crit. Rev. Environ. Sci. Technol. 35 (2005) 571–622.
[5] J.A. Cole, J.C. Kramlich, W.R. Seeker, M.P. Heap, Activation and reactivity of calcareous solvents towards sulfur dioxide, Environ. Sci. Technol. 19 (1985) 1065.
[6] L.E. Kallinikos, E.I. Farsari, D.N. Spartinos, N.G. Papayannakos, Simulation of the operation of an industrial wet flue gas desulfurization system, Fuel Process. Technol. 91 (2010) 1794–1802.
[7] D.J. Helfritch, P.L. Feldman, Flue gas SO_2/NO_x control by combination of dry scrubber and electron beam, Radiat. Phys. Chem. 24 (1984) 129–143.
[8] H.L. Gao, C.T. Li, G.M. Zeng, W. Zhang, L. Shi, S.H. Li, Y.N. Zeng, X.P. Fan, Q.B. Wen, X. Shu, Flue gas desulphurization based on limestone-gypsum with a novel wet-type PCF device, Sep. Purif. Technol. 76 (2011) 253–260.
[9] W.Z. Wu, B.X. Han, H.X. Gao, Z.M. Liu, T. Jiang, J. Huang, Desulfurization of flue gas: so$_2$ absorption by an ionic liquid, Angew. Chem. Int. Ed. 43 (2004) 2415–2417.
[10] J.H. Yang, S.M. Shih, C.I. Wu, C.Y.D. Tai, Preparation of high surface area $CaCO_3$ for SO_2 removal by absorption of CO_2 in aqueous suspensions of $Ca(OH)_2$, Powder Technol. 202 (2010) 101–110.
[11] I. Dahlan, K.T. Lee, A.H. Kamaruddin, A.R. Mohamed, Selection of metal oxides in the preparation of rice husk ash (RHA)/CaO sorbent for simultaneous SO_2 and NO removal, J. Hazard. Mater. 166 (2009) 1556–1559.
[12] X.Y. Zhang, G.S. Zhuang, J.M. Chen, Y. Wang, X. Wang, Z.S. An, P. Zhang, Heterogeneous reactions of sulfur dioxide on typical mineral particles, J. Phys. Chem. B 110 (2006) 12588–12596.
[13] S.J. Lee, S.Y. Jung, S.C. Lee, H.K. Jun, C.K. Ryu, J.C. Kim, SO_2 removal and regeneration of MgO-based sorbents promoted with titanium oxide, Ind. Eng. Chem. Res. 48 (2009) 2691–2696.
[14] L.S. Jae, H.K. Jun, S.Y. Jung, T.J. Lee, C.K. Ryu, J.C. Kim, Regenerable MgO-based SO_x removal sorbents promoted with cerium and iron oxide in RFCC, Ind. Eng. Chem. Res. 44 (2005) 9973–9978.
[15] M. Mehta, M. Mukhopadhyay, R. Christian, N. Mistry, Synthesis and characterization of MgO nanocrystals using strong and weak bases, Powder Technol. 226 (2012) 213–221.
[16] A.H. Chowdhury, I.H. Chowdhury, M.K. Naskar, A facile synthesis of grainy rod-like porous MgO, Mater. Lett. 158 (2015) 190–193.
[17] R. Sathyamoorthy, K. Mageshwari, S.S. Mali, S. Priyadharshini, P.S. Patil, Effect of organic capping agent on the photocatalytic activity of MgO nanoflakes obtained by thermal decomposition route, Ceram. Int. 39 (2013) 323–330.
[18] M. Waqif, A.M. Saad, M. Bensitel, J. Bachelier, O. Saur, J.C. Lavalley, Comparative study of SO_2 adsorption on metal oxides, J. Chem. Soc. Faraday Trans. 88 (1992) 2931–2936.
[19] Z. Wang, Current conditions and developing tendency of magnesite in China, China Non-Metal Min. Ind. Her. 1 (2006) 6–8.
[20] B. Feray, L. Oral, B. Bahar, S. Hanifi, Dissolution kinetics of natural magnesite in lactic acid solutions, Int. J. Min. Process. 80 (2006) 27–34.
[21] B. Bayrak, O. Lacin, F. Bakan, H. Sarac, Investigation of dissolution kinetics of natural magnesite in gluconic acid solutions, Chem. Eng. J. 117 (2006) 109–115.
[22] K. Sasaki, N. Fukumoto, S. Moriyama, T. Hirajima, Sorption characteristics of fluoride on to magnesium oxide-rich phases calcined at different temperatures, J. Hazard. Mater. 191 (2011) 240–248.
[23] N. Li, Formation, compressibility and sintering of aggregated MgO powder, J.

Mater. Sci. 24 (1989) 485–492.
[24] A.F. Moodie, C.E. Warble, MgO morphology and the thermal transformation of $Mg(OH)_2$, J. Cryst. Growth 74 (1986) 89–100.
[25] Y.X. Yun, X.X. Zhang, X.X. Zhao, J.X. Yao, J.Y. Jiang, Infrared absorption properties of SF6 gas-decomposition products SO2, H2S, HF and CO, High Volt. Eng. 39 (2013) 2651–2656.
[26] J. Przepiorski, A. Czyzewski, J. Kapica, D. Moszynski, B. Grzmil, B. Tryba, S. Mozia, A.W. Morawski, Low temperature removal of SO_2 traces from air by MgO-loaded porous carbons, Chem. Eng. J. 191 (2012) 147–153.
[27] Y. Liu, T.M. Bisson, H.Q. Yang, Z.H. Xu, Recent developments in novel sorbents for flue gas clean up, Fuel Process. Technol. 91 (2010) 1175–1197.
[28] J.V. Stark, D.G. Park, I. Lagadic, K.J. Klalunde, Nanoscale metal oxide particles/clusters as chemical reagents. unique surface chemistry on magnesium oxide as shown by enhanced adsorption of acid gases (sulfur dioxide and carbon dioxide) and pressure dependence, Chem. Mater. 9 (1996) 1904–1912.
[29] A.J. Goodsel, M.J. Low, N. Takezawa, Reactions of gasous pollutants with solids.II.infrared study of sorption of SO_2 on MgO, Environ. Sci. Technol. 6 (1972) 268–273.